Ceragenins and antimicrobial peptides kill bacteria through distinct mechanisms

Gabriel Mitchell[1§], Melanie R. Silvis[2], Kelsey C. Talkington[1], Jonathan M. Budzik[1,3], Claire E. Dodd[1], Justin M. Paluba[1], Erika A. Oki[1], Kristine L. Trotta[4], Daniel J. Licht[1], David Jimenez-Morales[5,6], Seemay Chou[4], Paul B. Savage[7], Carol A. Gross[2,8], Michael A. Marletta[1,9,10#] and Jeffery S. Cox[1#]

Running title: Ceragenins kill bacteria through a distinct mechanism

Keywords: Antibiotics, Gram-negative, Gram-positive, mycobacteria, CSA

[1]Department of Molecular and Cell Biology, University of California, Berkeley, USA.
[2]Department of Microbiology and Immunology, University of California, San Francisco, USA.
[3]Department of Medicine, University of California, San Francisco, USA.
[4]Department of Biochemistry and Biophysics, University of California, San Francisco, USA.
[5]Department of Medicine, Division of Cardiovascular Medicine, Stanford University, CA, USA.
[6]Department of Cellular and Molecular Pharmacology, University of California, San Francisco, USA.
[7]Department of Chemistry and Biochemistry, Brigham Young University, Provo, Utah, USA.
[8]Department of Cell and Tissue Biology, University of California, San Francisco, USA.
[9]Department of Chemistry, University of California, Berkeley, USA.
[10]California Institute for Quantitative Biosciences, University of California, Berkeley, USA.
[#]Corresponding authors: jeff.cox@berkeley.edu; marletta@berkeley.edu
§Current address: Open Innovation @ NITD, Novartis Institute for Tropical Diseases, Emeryville, CA, USA.

ABSTRACT

Ceragenins are a family of synthetic amphipathic molecules designed to mimic the properties of naturally-occurring cationic antimicrobial peptides (CAMPs). Although ceragenins have potent antimicrobial activity, whether their mode of action is similar to that of CAMPs has remained elusive. Here we report the results of a comparative study of the bacterial responses to two well-studied CAMPs, LL37 and colistin, and two ceragenins with related structures, CSA13 and CSA131. Using transcriptomic and proteomic analyses, we found that *Escherichia coli* responds similarly to both CAMPs and ceragenins by inducing a Cpx envelope stress response. However, whereas *E. coli* exposed to CAMPs increased expression of genes involved in colanic acid biosynthesis, bacteria exposed to ceragenins specifically modulated functions related to phosphate transport, indicating distinct mechanisms of action between these two classes of molecules. Although traditional genetic approaches failed to identify genes that confer high-level resistance to ceragenins, using a Clustered Regularly Interspaced Short Palindromic Repeats interference (CRISPRi) approach we identified *E. coli* essential genes that when knocked down modify sensitivity to these molecules. Comparison of the essential gene-antibiotic interactions for each of the CAMPs and ceragenins identified both overlapping and distinct dependencies for their antimicrobial activities. Overall, this study indicates that while some bacterial responses to ceragenins overlap with those induced by naturally-occurring CAMPs, these synthetic molecules target the bacterial envelope using a distinctive mode of action.

IMPORTANCE

The development of novel antibiotics is essential since the current arsenal of antimicrobials will soon be ineffective due to the widespread occurrence of antibiotic resistance. Development of naturally-occurring cationic antimicrobial peptides (CAMPs) for therapeutics to combat antibiotic resistance has been hampered by high production costs and protease sensitivity, among other factors. The ceragenins are a family of synthetic CAMP mimics that kill a broad spectrum of bacterial species but are less expensive to produce, resistant to proteolytic degradation and have been associated with low levels of resistance. Determining how ceragenins function may identify new essential biological pathways of bacteria that are less prone to development of resistance and will further our understanding of the design principles for maximizing the effects of synthetic CAMPs.

INTRODUCTION

Our current arsenal of antibiotics will soon be ineffective against the simplest bacterial infections due to the continued spread of antibiotic resistance (AR) (1). AR has been identified in virtually all bacterial species of clinical relevance, including Gram-positive and Gram-negative bacteria as well as mycobacteria (2). Despite the threat that AR represents to global health, there is a lack in the development of antimicrobials with innovative mechanisms of action (3-5). A better understanding of the fundamental principles of how antibiotics kill microbes and how AR develops will help break the futile cycle of antibiotic development and microbial evolution.

Antimicrobial peptides are structurally diverse molecules expressed in a wide array of organisms that directly kill microbes, including bacteria (6, 7). Many antimicrobial peptides, such as the class of cationic antimicrobial peptides (CAMP), rapidly kill bacteria by disrupting membranes although other mechanisms of action were also suggested (7-9). The potential of using CAMPs to treat AR infections has become a research focus due to their action against a broad spectrum of pathogens, their selectivity toward microbial membranes and the low appearance of resistance (6, 10). Despite some progress in this area, significant barriers to CAMP therapeutic development include high production costs, toxicity, susceptibility to proteolytic degradation and activation of allergic responses (6, 10).

Ceragenins are a family of synthetic amphipathic molecules derived from cholic acid designed to mimic the activity of endogenous CAMPs (11, 12). These molecules are

inexpensive to manufacture and are not susceptible to proteolysis, making them an attractive alternative to peptide-based synthetic CAMPs. Importantly, ceragenins have antimicrobial activity against a broad spectrum of microbes, which include both Gram-negative and Gram-positive bacteria (11, 13). High-level resistance to ceragenins is seemingly difficult to acquire in the lab as attempts to isolate ceragenin-resistance bacterial mutants failed in the Gram-positive bacterium *Staphylococcus aureus* and identified only modest and unstable resistance in Gram-negatives (14). Although ceragenins were designed as CAMP mimics and can depolarize bacterial membranes (15), the inability to identify bona-fide ceragenin-resistant bacterial mutants represents a major barrier in understanding their mechanism of action.

Here we take a comparative approach using a combination of transcriptomic, proteomic and genetic approaches to compare the bacterial responses to treatment with ceragenins and two well-studied CAMPs. The results of this study suggests that ceragenins kill bacteria by disrupting the bacterial envelope through a distinctive mode of action from naturally-occurring CAMPs. We also show, for the first time, that ceragenins have activity against mycobacteria despite their distinctive cell wall architecture.

MATERIALS AND METHODS

Antimicrobial compounds. CSA13 and CSA131 (16) as well as CSA44 and CSA144 (17) were prepared as described previously and solubilized at 10 mg/mL in sterile distilled and deionized (DD) water. LL37 (Anaspec, Fremont, California, USA), colistin (Sigma-Aldrich, St-Louis, MO, USA) and ciprofloxacin (MP Biomedicals, Irvine, California, USA) were solubilized at 10 mg/mL in sterile DD water. Erythromycin (Sigma-Aldrich) was solubilized at 10mg/mL in ethanol. Antimicrobial compounds were aliquoted and stored at -20^{o} C. Freeze-thaw cycles of stock solutions were limited to three times.

Bacterial strains, growth conditions. *E. coli* MG1655 (18), *L. monocytogenes* 10403S (19)**,** *M. marinum* strain M (20), *M. smegmatis* mc^{2}155 (21) and *M. tuberculosis* Erdman (20) were as previously described. *M. avium* mc^{2}2500 is a clinical strain isolated from an acquired immunodeficiency syndrome (AIDS) patient with pulmonary disease and predominantly formed a smooth/transparent colony morphotype on solid agar (22). *M. avium* mc^{2}2500D is an isogenic, laboratory-derived strain with an opaque colony morphotype. *E. coli* and *L. monocytogenes* were routinely grown on Mueller-Hinton agar (MHA) (BD, Franklin Lakes, New Jersey, USA) plates or in cation-adjusted Mueller-Hinton (CAMH) (BD) broth and on Brain-heart infusion agar (BHIA) (Becton Dickinson) plates or in Brain-heart infusion (BHI) (BD) broth, respectively. *M. avium* and *M. tuberculosis* were cultured in Middlebrook 7H9 (BD) broth containing 0.5% glycerol, 10 % Oleic Albumin Dextrose Catalase (OADC) (Sigma-Aldrich) and 0.05% Tween-80. *M. marium* was cultured in Middlebrook 7H9 broth containing 0.5% glycerol,

10 % OADC and 0.2% Tween-80. *M. smegmatis* was grown on Middlebrook 7H10 (BD) plates or Middlebrook 7H9 plates containing 0.5% glycerol, 0.5% dextrose and 0.2% Tween-80, unless otherwise stated. All bacterial strains were grown at 37^{o} C, except from *M. marinum*, which was grown at 30^{o} C. Liquid cultures were incubated with shaking, unless otherwise stated.

Antibiotic susceptibility testing. Minimal inhibitory concentrations (MICs) of antimicrobial compounds against *E. coli* and *L. monocytogenes* were determined by a broth microdilution technique following the recommendations of the Clinical and Laboratory Standards Institute (CLSI) (23), except that BHI was used to perform assays on *L. monocytogenes*. Antibiotic quality control experiments were performed using *E. coli* ATCC25922 (ATCC, Manassas, VA, USA). A similar protocol using extended incubation periods was used to determine MICs against *M. avium* (10 days), *M. marinum* (5 days), *M. smegmatis* (3 days) and *M. tuberculosis* (14 days). For the determination of MICs using mycobacterial species, plates were placed in a vented container containing damp wipes to minimize evaporation.

Time-kill experiments. Time-kill experiments were performed to characterize the effect of compounds on bacterial growth and survival. Bacteria were inoculated at 10^{5}-10^{6} CFU/mL in liquid media in the absence or presence of antibiotics at the following concentrations: *E. coli*, 0.5 µg/mL colistin, 64 µg/mL LL37, 4 µg/mL CSA13 and 4 µg/mL CSA131; *L. monocytogenes*, 2 µg/mL CSA13, 2 µg/mL CSA131, 2 µg/mL ciprofloxacin and 0.25 µg/mL erythromycin; *M. smegmatis*, 0.5 µg/mL CSA13 and 0.5

µg/mL ciprofloxacin. Bacterial cultures were grown at 37° C with shaking and the number of CFU/mL was determined at several time points. Plates without Tween-80 were used for the CFU determination of *M. smegmatis* cultures.

Serial passage experiments. Serial passage of bacteria in presence of sub-inhibitory concentrations was performed as previously described (14, 24). Experiments were performed in CAMH or BHI broth for *E. coli* and *L. monocytogenes*, respectively. In few cases, bacteria growing at the two highest sub-inhibitory concentrations of antimicrobial had to be combined in order to get an inoculums of 10^5-10^6 CFU/mL.

Preparation and sampling of bacterial cultures for transcriptomic profiling. A single colony of *E. coli* MG1655 was inoculated into CAMH broth and incubate 16-18 h at 37° C with shaking. Cultures were diluted in fresh media to an A_{600nm} of 0.1, incubated at 37° C with shaking until an A_{600nm} of 0.8-1.0 (~2h) and antibiotics were added to each cultures, which were further incubated for 1 h at 37° C with shaking. Antibiotic were adjusted to concentrations having similar impact on *E. coli* growth for that particular, higher bacterial density, culture format (i.e. 4 µg/mL colistin, 8 µg/mL CSA13, 8 µg/mL CSA131 and 256 µg/mL LL37). Cultures samples were then mixed 1:2 with RNA Protect Bacteria Reagent (QIAGEN, Germantown, Maryland, USA), vortexed immediately for 5 seconds and incubated for 5 min at room temperature. The bacterial suspensions were centrifugated for 10 min at 5,000 × g, supernatants discarded and pellets were stored few days at -80° C before proceeding to RNA extraction.

RNA purification and sequencing. Bacterial pellets were resuspended in 100 µL of 10 mM Tris, 1 mM EDTA, pH 8.0 buffer containing 10 mg/mL lysozyme (Sigma-Aldrich). 2.5 µL of 20 mg/mL Proteinase K (NEB, Ipswich, Massachusetts, USA) was added and samples were incubated at room temperature for 10 min, with frequent mixing. Samples were combined with 0.5 µL of 10% SDS and 350 µL of Lysis Buffer (Ambion life technologies, Invitrogen, Carlsbad, California, USA) containing β-mercaptoethanol, vortexed and the lysate was transferred into a 1.5 mL RNase-free microcentrifuge tube. Samples were then passed 5 times through an 18-21-gauge needle and centrifuged at 12,000 × g for 2 minutes at room temperature. Supernatants were transferred to a new 1.5 mL RNase-free microcentrifuge tube before proceeding to the washing and elution steps described in the PureLink RNA Mini Kit (Ambion life technologies). Samples were treated with DNase (NEB) for 15 min at 37^{o} C in a volume of 50 µL and 5 µL of 25 mM EDTA was added. Samples were further incubated 10 min at 75^{o} C and quickly placed on ice before being cleaned and re-eluted using the RNA Clean & Concentrator kit (Zymo Research, Irvine, CA, USA) and stored at -80^{o} C. The quality and the quantity of each RNA samples was analyzed by the UC Berkeley QB3 facility using a bioanalyzer and the Qubit technology. RNA samples were sequenced and preliminary analyzed by the UC Davis Genome Center and the UC Davis Bioinformatics Core.

Analysis of RNAseq data. The differential expression analyses were conducted using the limma-voom Bioconductor pipeline (25) (EdgeR version 3.20.9, limma version 3.34.9) and R 3.4.4 by the UC Davis Bioinformatics Core. The multidimensional plot was created using the EdgeR function plotMDS. Pathway analyses were performed using

DAVID Bioinformatics Resources 6.8 (26, 27). Only annotation terms from the following databases were included: UP (UniProt) Keywords, COG (Cluster of Orthologous Groups) Ontology, GO (Gene Ontology for Biological process, Molecular function and Cellular component) and KEGG (Kyoto Encyclopedia of Genes and Genomes). Venn diagram analyses were performed using the tool provided on the Bioinformatics & Evolutionary Genomics website of Ghent University (28). Promoter and regulatory binding analyses were performed using the Gene Expression Analysis Tools (29). Only one repeated binding sites and promoters was considered for each gene for any specific transcription factors. Lists of genes to be included in specific regulons were retrieved from the RegulonDB Database (30). Fold changes for few transcripts of regulons CpxR (*cpxQ*, *csgC*, *cyaR*, *efeU*, *rprA*, *rseD*), PurR (*codA*, *codB*) and PhoB (*cusC*, *phnE*, *prpR*) were not included in this analysis. The information related to the expected activity (induction and/or repression) of each transcription factor on specific genes were also retrieved from the RegulonDB Database.

Protein extraction and peptide preparation from *E. coli* cultures. A single colony of *E. coli* MG1655 was inoculated into CAMH broth and incubate 16-18 h at 37^{o} C with shaking. Cultures were diluted in fresh media to an A_{600nm} of 0.1, incubated at 37^{o} C with shaking until an A_{600nm} of 0.8-1.0 (~2 h) and antibiotics (4 µg/mL colistin or 8 µg/mL CSA13) were then added to each cultures, which were further incubated for 3 h at 37^{o} C with shaking. Protein were extracted, digested and desalted, as previously described (31), with few modifications. Briefly, 23 mL of bacteria cultures were washed twice in cold PBS and resuspended in 4 mL of lysis buffer (8 M urea, 150 mM NaCl, 100 mM

ammonium bicarbonate, pH 8) containing Roche mini-complete protease inhibitor EDTA-free and Roche PhosSTOP (1 tablet of each per 10 mL of buffer) (Roche, Basel, Switzerland). Samples (on ice) were then sonicated 10 times with a Sonics VibraCell probe tip sonicator at 7 watts for 10 seconds. Insoluble precipitates were removed from lysates using a 30 min centrifugation at ~16,100 × g at 4^{o} C and the protein concentration of each lysates was determined using the microplate procedure of the Micro BCA^{TM} Protein Assay Kit (Thermo Fischer Scientific, Emeryville, CA, USA). Clarified lysates (1 mg each) was reduced with 4 mM tris(2-carboxyethyl)phosphine for 30 min at room temperature, alkylated with 10 mM of iodoacetamide for 30 min at room temperature in the dark and quenched with 10 mM 1,4-dithiothreitol for 30 min at room temperature in the dark. Samples were diluted with three volumes of 100 mM ammonium bicarbonate, pH 8.0, and incubated with 10 µg of sequencing grade modified trypsin (Promega, Madison, WI, USA) while rotating at room temperature for 18 hours. Trifluoroacetic acid (TCA) was then added to a final concentration of 0.3% to each samples, followed by 1:100 of 6M HCl and the removal of insoluble material by centrifugation at ~2,000 × g for 10 min. SepPak C18 solid-phase extraction cartridges (Waters, Milford, MA, USA) were activated with 1 mL of 80% acetonitrile (ACN), 0.1% TFA, and equilibrated with 3 mL of 0.1% TFA. Peptides were desalted by applying samples to equilibrated columns, followed by a washing step with 3 mL of 0.1% TFA and elution with 1.1 mL of 40% ACN, 0.1% TFA. The subsequent global protein analysis was performed using 10 µg of each desalted peptide sample.

Liquid chromatography, mass spectroscopy and label-free quantification. Peptides were analyzed using liquid chromatography and mass spectroscopy, as previously described (31). Mass spectrometry data was assigned to *E. coli* sequences and MS1 intensities were extracted with MaxQuant (version 1.6.0.16) (32). Data were searched against the *E. coli* (strain K12) protein database (downloaded on November 6, 2018). MaxQuant settings were left at the default except that trypsin (KR|P) was selected, allowing for up to two missed cleavages. Data were then further analyzed with the artMS Bioconductor package (33), using the MSstats Bioconductor package (version 3.14.1) (34) and the artMS version 0.9. Contaminants and decoy hits were removed, and samples were normalized across fractions by median-centering the $\log_2$-transformed MS1 intensity distributions. The MSstats group comparison function was run with no interaction terms for missing values, no interference, unequal intensity feature variance as well as restricted technical and biological scope of replication. Log_2(fold change) for protein/sites with missing values in one condition but found in > 2 biological replicates of the other condition of any given comparison were estimated by imputing intensity values from the lowest observed MS1-intensity across samples (33), and P_{values} were randomly assigned between 0.05 and 0.01 for illustration purposes.

Identification of genetic determinants of resistance to antibiotics using CRISPRi. A pooled CRISPRi library of strains with inducible knockdown of genes predicted to be essential (FIG. S1) was used to study the genetic determinants of resistance to CAMPs and ceragenins. To quantify the antibiotic sensitivity of each CRISPRi strain, the relative proportion of each sgRNA spacer in the mixed population was enumerated by deep

sequencing, after 15 doublings in presence of saturating IPTG and 0.031 µg/mL colistin, 12 µg/mL LL37, 0.5 µg/mL CSA13 and 0.25 µg/mL CSA131. Briefly, a single glycerol stock of the pooled library was fully thawed, inoculated into 10 mL LB at 0.01 A_{600}, and grown for 2.5 hr (final ~0.3 A_{600}) at 37^{o} C with shaking. This culture was collected (10 mL, t0) and used to inoculate replicate 4 mL LB cultures (+/- 1mM IPTG and antibiotics) at 0.01 A_{600}, which were then repeatedly grown 130 min to 0.3 A_{600} (5x doublings) and back-diluted to 0.01 for a total of 3 times (15x doublings). At the endpoint, cultures were collected (4 mL, t15) by pelleting (9000 × g for 2 min) and stored at -80^{o} C. The following day, genomic DNA was extracted using the DNeasy Blood & Tissue kit (Qiagen #69506) with the recommended pre-treatment for Gram-negative bacteria and a RNAse A treatment. sgRNA spacer sequences were amplified from gDNA using Q5 polymerase (NEB) for 14x cycles using custom primers containing TruSeq adapters and indices, followed by gel-purification from 8% TBE gels. All sequencing was performed at the Chan Zuckerberg Biohub on the Illumina NextSeq platform using Single End 50bp reads.

Design of the sequencing libraries was optimized to enable multiplexing of many samples and to ensure diversity during cluster generation on the Illumina platform. Custom primers were used to generate the sequencing library that incorporated a second barcode (4bp) to be read in Read 1 (SeqLib.A.F and SeqLib.B.F in Fig. S1). In combination with the TruSeq barcode incorporated by the opposite primer (SeqLib.R in Fig. S1), this enabled the samples to be effectively dual-indexed. In preparing the sequencing libraries, samples were split into two types, Library Type A and Library Type

B, which differ in the offset position of the TruSeq Read 1 primer used for sequencing (Fig. S1). Briefly, Library Type A introduces a 2bp offset, as such that, when libraries of Type A and Type B are sequenced on the same flowcell, diversity of sequencing reads is ensured throughout the read length, which includes the spacer region (variable sequence) and the promoter region (identical sequence).

Spacer sequences were extracted from FASTQ files and counted by exact matching to expected library spacers. For each treatment condition, the counts tables from each biological replicate were used as inputs for DESeq2 to calculate the change in abundance (Log_2FC) and statistical significance (P_{value} and adjusted P_{value}).

Determination of LogP values. LogP values (partition coefficient) were determined using Chemicalize from ChemAxon (Escondido, California, USA).

Preparation of graphs. GraphPad Prism software (v.7.00) was used to generate graphs and performed statistical tests. Number of independent experiments are indicated in each figure legend.

RESULTS

Susceptibility of bacteria to CAMPs and ceragenins. Minimal inhibitory concentrations (MIC) for the CAMPs colistin and LL37 as well as two ceragenin compounds, CSA13 and CSA131 (see structures in FIG. 1A), were determined against the Gram-negative bacterium *E. coli*, the Gram-positive bacterium *L. monocytogenes* and several mycobacterial species (i.e. *M. avium*, *M. marinum*, *M. smegmatis* and *M. tuberculosis*) (FIG. 1B-1H and Table S1). The fluoroquinolone antibiotic ciprofloxacin (CIP, which inhibits DNA gyrase) was included as a positive control. As expected, colistin, which requires binding to LPS for activity (35), was active against *E. coli* (FIG. 1B), but not against *L. monocytogenes* (FIG. 1C) and each of the mycobacterial species (FIG. 1D-1H). Interestingly, LL37 was active against *E. coli* (FIG. 1B) and *L. monocytogenes* (FIG. 1C) but had no detectable activity against mycobacterial species (FIG. 1D-1H). The ceragenins CSA13 and CSA131 were also active against both *E. coli* (FIG. 1B) and *L. monocytogenes* (FIG. 1C). In contrast to colistin and LL37, the ceragenins had activity against mycobacteria, although the MICs varied between species (FIG. 1D-1H). While *M. smegmatis* was highly susceptible to CSA13 and CSA131 (FIG. 1G), both compounds were less active against the slower-growing species *M. avium* (FIG. 1D and 1E), *M. marinum* (FIG. 1F) and *M. tuberculosis* (FIG. 1H). Similar trends in MIC values for *E. coli*, *L. monocytogenes* and *M. smegmatis* were observed with two other ceragenin compounds, CSA44 and CSA144 (See Table S1), which further confirmed that ceragenins have antimicrobial activity against mycobacteria. Overall, these results demonstrate that the spectrum of activity of ceragenins is broader than colistin and LL37, indicating different requirements for activity.

Ceragenins are bactericidal. To determine if ceragenins kill all three types of bacteria, we performed kill-curve experiments at inhibitory concentrations (~1-2 × MICs) of the molecules (FIG. 1I-1K). Ceragenins (CSA13 or CSA131) killed *E. coli* (FIG. 1I), *L. monocytogenes* (FIG. 1J) and *M. smegmatis* (FIG. 1K), although some bacterial cultures recovered during this time course. These results confirmed that ceragenins act on bacteria through a bactericidal mechanism.

Serial passage of *E. coli* and *L. monocytogenes* in the presence of sub-inhibitory concentrations of ceragenins. Isolation and characterization of antibiotic-resistant bacteria could provide insight into the mode of action of ceragenins. As such, the generation of ceragenin-resistant bacteria was attempted by performing serial passaging experiments with *E. coli* and *L. monocytogenes* in the presence of sub-inhibitory concentrations of ciprofloxacin, CSA13 and CSA131 (FIG. 1L and 1M). In contrast to ciprofloxacin-exposed bacteria, *E. coli* and *L. monocytogenes* bacteria exposed to ceragenins did not give rise to stable resistance. The generation of spontaneous *M. smegmatis* mutants resistant to CSA13 was also attempted, but no CSA13-resistant bacteria were recovered, although bacteria resistant to ciprofloxacin and rifampicin were isolated from parallel control experiments (data not shown). These results confirmed that resistance to ceragenins is infrequent (14) and does not emerge *in vitro* under conditions known to generate resistant mutants against antibiotics.

Transcriptional response of *E. coli* exposed to ceragenins. The transcriptional response of bacteria to antibiotics was analyzed to gain insights into the mechanism of action of CAMPs and ceragenins, as similarly reported for other antibacterial compounds (36, 37). More specifically, we determined the global transcriptional responses of *E. coli* exposed to colistin, LL37, CSA13 and CSA131 using RNAseq. Bacteria were grown to log phase and treated with supra-MIC concentrations of antibiotics for one hour before being harvested for RNA extraction and sequencing (see Materials and Methods). Plots of the normalized number of reads per gene showed an excellent correlation (R = 0.965-0.999) between biological replicates for each of the conditions tested (FIG. 2A-2D), demonstrating the reproducibility of the method. Hundreds of statistically significant changes in gene expression (defined by absolute $\log_2$ fold change >1 and adjusted P_{value} < 0.05) following exposure of bacteria to colistin, LL37, CSA13 and CSA131 were measured (FIG. 2E-2H and Data Set S1). These results validated our RNAseq approach for the analysis of the transcriptional response of *E. coli* to antibiotics.

The global transcriptional responses of *E. coli* in response to CAMPs and ceragenins was analyzed using a multidimensional scaling analysis (FIG. 2I). Interestingly, while transcriptional responses of bacteria to CAMPs were extremely similar, the response to CSA13 and CSA131 were not only distinct from these CAMPs, but also distinct from each other. Those trends were corroborated using pathway analysis that showed the enrichment of annotation terms associated with the outer membrane (e.g. lipopolysaccharide and colanic acid) in genes up-regulated by CAMPs, but not ceragenins, (FIG. 2J and Data Set S2) as well as the enrichment of terms associated with

translation in genes down-regulated by CSA13, but not CSA131 (FIG. 2K and Data Set S2). While the two ceragenins are structurally quite similar, the addition of four methylene groups to the CSA13 carbon chain to create CSA131 significantly increases the hydrophobicity of the molecule, increasing the partition coefficient from $LogP_{CSA13}$ = 5.51 to $LogP_{CSA131}$ = 7.29 (see Materials and Methods), which likely contributes to differences in antibacterial activities. Overall, these results showed that transcriptional responses of *E. coli* to the naturally-occurring CAMPs colistin and LL37 are similar, but differ from the response to ceragenins. These results also suggested that *E. coli* responds differently to the structurally related ceragenin compounds, CSA13 and CSA131.

Identification of pathways defining the transcriptional response of *E. coli* to ceragenins. Pathway analysis of genes modulated by more than one compound was performed to further define transcriptional responses to CAMPs and ceragenins. The Venn diagram in Figure 3A visualizes the extent of overlap of the individual *E. coli* genes that had significant increases in mRNA abundance upon treatment with each of the molecules. In particular, 86 genes were induced in all four conditions, 68 were upregulated specifically during CAMP treatment while 57 were induced by the ceragenins (FIG. 3A and Data Set S3). The annotation term “signal” was significantly enriched among the genes up-regulated by all antibiotics (FIG. 3A and Data Set S3), which might be indicative of a common response to CAMPs and ceragenins. Interestingly, this group included genes involved in the membrane stress response such as *spy*, *degP* and *cpxP* (38) (Fig. 3B). Consistent with results from FIG. 2, genes specifically up-regulated in bacteria exposed to CAMPs were significantly associated with annotation

terms related to LPS/colanic acid biosynthesis and included genes such as *wzc*, *wcaE* and *cpsB* (FIG. 3A, 3B and Data Set S3). Interestingly, genes specifically up-regulated in bacteria exposed to ceragenins were significantly associated with the annotation term "phosphate transport" (FIG. 2J, FIG. 3A and Data Set S3) and include genes encoding the major phosphate-responsive regulators PhoR and PhoB (FIG. 3B). Overall, these results suggested that *E. coli* responds to CAMPs and ceragenins by upregulating genes involved in signaling and response to membrane stress. These results also showed that while exposure of *E. coli* to CAMPs induces the expression of genes related to LPS/colanic acid biosynthesis, exposure to ceragenins induces the expression of genes involved in phosphate transport.

For genes with mRNA levels that decreased during these treatments, 101 were down-regulated by all antibiotics, 19 by CAMPs, and 70 by ceragenins (FIG. 3C and Data Set S3). Pathway analysis identified enrichment of terms related to amino acids and nucleotide metabolism in genes down-regulated following exposure to all antibiotics (FIG. 3C and Data Set S3). This finding was corroborated by the finding that genes related to purine and pyrimidine biosynthesis (e.g. *pyrB*, *purM* and *purT*) were among the most significantly down-regulated genes by these molecules (FIG. 3D), which is consistent with our pathway analysis (FIG. 2K). Whereas no annotation terms were significantly enriched for genes only down-regulated by CAMPs, genes down-regulated by ceragenins showed an enrichment for genes involved in oligopeptide/dipeptide transport such as *dppD* and *dppA* (FIG. 3C, FIG 3D and Data Set S3). Although the reason for the downregulation of genes involved in peptide transport in *E. coli* exposed to

ceragenins is unknown, these results suggested that bacteria exposed to CAMPs and ceragenins respond by downregulating genes involved in metabolic pathways.

Identification of cis-acting elements that regulate the transcriptional response of *E. coli* to ceragenins. To determine which signal transduction pathways control the transcriptional responses to CAMPs and ceragenins, the DNA sequences immediately 5' of genes with significantly altered mRNA levels were analyzed for the presence of cis-acting promoter and operator sequences known or predicted to recruit transcription factors (29). Interestingly, genes up-regulated following exposure to each of the molecules (FIG. 4A and Data Set S4) were associated with cis-acting elements interacting with the response regulator CpxR of the CpxA/CpxR two-component regulatory system (enrichment of 11.63%; 10 out of 86 genes), which responds to envelope stress (39) and is consistent with the upregulation of the CpxR-regulon genes *spy*, *degP* and *cpxP* (FIG. 3B). This analysis also showed enrichment for genes associated with cis-acting elements binding the primary sigma factor σ^D (40), also involved in the redistribution of the RNA polymerase in response to osmotic stress (41), the alternative sigma factor σ^E that coordinates the envelope stress response (39, 42, 43), and the alternative sigma factor σ^H, which controls the expression of heat shock genes as well as genes involved in membrane functionality and homeostasis (44) (FIG. 4A). Genes down-regulated following exposure to all antibiotics were associated with the presence of binding sites for the HTH-type transcriptional repressor PurR (FIG. 4B and Data Set S4), which regulates genes involved in the de novo synthesis of purine and pyrimidine nucleotides (45, 46) and corroborates our above analysis (FIG. 2K, 3C and 3D). Overall,

443 these results suggested that CAMPs and ceragenins perturb the bacterial envelope and
444 trigger the CpxA/CpxR system. These results also suggested that PurR down-regulates
445 the expression of genes involved in the biosynthesis of purine and pyrimidine following
446 the exposure of *E. coli* to CAMPs and ceragenins.
447
448 **Expression of the CpxR, PurR, RcsA and PhoB regulons in *E. coli* exposed to**
449 **ceragenins.** To further confirm a role for CpxR and PurR in the response of *E. coli* to
450 CAMPs and ceragenins, the expression of the CpxR and PurR regulons was analyzed in
451 more detail (FIG. 5A-B and Data Set S4). The heat map of the CpxR regulon showed a
452 consistent regulation of several genes in bacteria exposed to all four compounds (e.g.
453 *cpxP*, *degP*, *dsbA* and *spy*) (FIG. 5A) and corroborates our results described above (FIG.
454 3B and 4A). Also consistent with our findings described above (FIG. 2K, 3C, 3D and
455 4B), the heat map of the PurR regulon (FIG. 5B) showed downregulation of most genes
456 reported to be repressed by this transcription factor. These results confirmed that the
457 expression of the CpxR and PurR regulons are modulated in *E. coli* exposed to CAMPs
458 and ceragenins.
459
460 Our expression analysis led us to also focus on the RcsA and PhoB regulons to
461 gain insight into the differential regulation of genes involved in the biosynthesis of
462 colonic acid and phosphate transport, respectively (FIG. 5C-D and Data Set S4). RcsA
463 regulates the expression of genes involved in colanic acid biosynthesis (39), a pathway
464 that was up-regulated in *E. coli* exposed to CAMPs, but not ceragenins (FIG. 2J, 3A and
465 3B). Accordingly, the heat map of the RcsA regulon showed a marked modulation of this

466 pathway in *E. coli* exposed to CAMPs in comparison to ceragenins (FIG. 5C). The
467 phosphate regulon transcriptional regulatory protein PhoB regulates the expression of
468 genes involved in phosphate transport (47) and is up-regulated in *E. coli* following
469 exposure to ceragenins, but not CAMPs (FIG. 2J, 3A and 3B). Accordingly, the heat map
470 of the PhoB regulon showed partial but specific induction in bacteria exposed to
471 ceragenins (FIG. 5D). More specifically, upregulation of the *phn C-phnP* operon, the
472 *pstSCAB-phoU* operon as well as a trend for other *pho* genes (e.g. *phoB* and *phoR*) and
473 the phosphate starvation-inducible *psiEF* genes were specifically observed in bacteria
474 exposed to ceragenins (FIG. 5D). These results suggested that the specific upregulation of
475 genes involved in colanic acid biosynthesis and phosphate transport in bacteria exposed
476 to colistin/LL37 and ceragenins are mediated by RcsA and PhoB, respectively.
477
478 **Proteomic response of *E. coli* exposed to colistin and CSA13.** To determine if the
479 changes in mRNA levels in response to the molecules led to changes in the proteome, we
480 measured global protein abundance in bacteria exposed to colistin and CSA13 by mass
481 spectrometry-based proteomics. *E. coli* cultures were grown to log phase and treated with
482 supra-MIC concentrations of antibiotics before protein extraction, peptide preparation
483 and peptide quantification (see Materials and Methods). Approximately 1800 unique
484 proteins were detected for each biological replicate (FIG. 6A) and the number of unique
485 peptides identified showed an excellent correlation between biological replicates (FIG.
486 6B). Several statistically significant changes in protein expression (absolute $\log_2$ fold
487 change >1 and adjusted $P_{value} < 0.05$) were observed following exposure of *E. coli* to
488 colistin (FIG. 6C) and CSA13 (FIG. 6D) (see Data Set S5). The dataset showed that *E.*

489 *coli* exposed to both colistin and CSA13 up-regulated the proteins DegP, Spy and YepE,
490 which are known members of the Cpx regulon (38) that were strongly up-regulated at the
491 transcriptional level following exposure to CAMPs and ceragenins (FIG. 5A). The
492 dataset also showed the modulation of proteins involved in colanic acid biosynthesis (e.g.
493 Ugd and WcaG) or related to the PhoB regulon (e.g. PstB and PstS) in bacteria exposed
494 to colistin or CSA13, respectively, which also corroborate our transcriptional data (FIG.
495 5C and 5D). Then, similarly to our transcriptional analysis, the proteomic data showed a
496 common induction of the Cpx envelope stress response, but also the specific induction of
497 proteins involved in colanic acid biosynthesis by colistin as well as the modulation of
498 members of the PhoB regulon by CSA13.
499
500 Annotation term enrichment analysis was performed on the proteomic dataset in
501 order to identify pathways significantly modulated in bacteria exposed to colistin and
502 CSA13 (see Data Set S6). Similar to our transcriptional results (FIG. 2J), the colanic acid
503 pathway was significantly enriched among proteins up-regulated by colistin, but not
504 CSA13 (FIG. 6E). A heat response signature was significantly enriched among proteins
505 uregulated by CSA13, but not colistin (FIG. 6E), corroborating the transcriptional
506 upregulation of genes associated with cis-acting elements for σ^H (FIG. 4A). In addition,
507 while pathways associated with the periplasm were enriched among proteins down-
508 regulated by both colistin and CSA13, the outer membrane pathway was significantly
509 enriched among proteins down-regulated by colistin, but not by CSA13 (FIG. 6E).
510 Overall, these results confirmed that *E. coli* responds distinctly to colistin and CSA13,
511 although both compounds modulated proteins associated with the bacterial envelope.

512 These results also confirmed findings from the transcriptional analysis and showed that
513 colistin and CSA13 modulate the colanic acid and the response to heat pathways,
514 respectively.
515
516 **Identification of genetic determinants of resistance to ceragenins in *E. coli*.** Our
517 inability to identify ceragenin-resistant *E. coli* mutants (FIG. 1L and 1M) is consistent
518 with results previously published by Pollard *et al.* (14), indicating that resistance to
519 ceragenins emerges infrequently in culture despite strong selective pressure. This
520 suggests that ceragenins either have multiple essential targets or affect cellular structures
521 that are immutable. Thus, traditional genetic approaches to identify the target(s) of
522 ceragenins has not been feasible. In order to gain insight into the genetic determinants of
523 ceragenin action, we employed an alternative genetic approach that utilizes Clustered
524 Regularly Interspaced Short Palindromic Repeats interference (CRISPRi) to reduce
525 expression of genes in *E. coli* (FIG. 7A). As demonstrated previously, this approach
526 allows for partial knockdown of essential *E. coli* genes, practically creating hypomorphic
527 alleles that have reduced function but still promote cell viability (48, 49). By combining
528 these genetic perturbations with subinhibitory concentrations of antibiotics and by
529 measuring the effects on bacterial fitness, we sought to identify functional interactions
530 between bacterial pathways and antibiotic stress.
531
532 We screened a pooled library of inducible essential gene knockdown strains
533 grown with or without subinhibitory concentrations of CAMPs or ceragenins (FIG. 7B).
534 To evaluate the fitness of each individual CRISPRi knockdown within the complex

535 population, we used deep sequencing to measure the relative abundance of guide
536 sequences during the different culturing conditions (see Materials and Methods and
537 FIG.S1). Fold changes in abundance (Log_2FC) in response to CAMPs and ceragenins
538 were calculated in comparison to the control condition for each knockdown strain, and
539 significantly resistant or sensitized strains (defined by absolute $\log_2$ fold change > 0.5 and
540 an adjusted $P_{value} < 0.05$) were identified for each of the compounds (FIG. 7C-7F and
541 Data Set S7). Interestingly, the CRISPRi guides in the sensitized or enriched strains for
542 one or several treatments predominantly targeted genes involved in the bacterial
543 envelope, consistent with our earlier results that both CAMPs and ceragenins affect the
544 bacterial envelope.
545
546 The changes in abundance for the genes identified above were further analyzed
547 and compared between treatments (FIG. 7G). Genes involved in the LPS biosynthetic
548 pathways were predominant in these screens, and knockdown of lipid-A-disaccharide
549 synthase LpxB (50) sensitized *E. coli* to all the compounds, highlighting again the
550 bacterial surface as a common site of action for CAMPs and ceragenins. Silencing of the
551 LPS transport genes *lptB* and *lptF* (51) led to sensitivity to colistin, LL37 and CSA131,
552 but not to CSA13, which corroborates the above transcriptomic data (FIG. 2I-K) and
553 again suggests distinctive mechanisms of action for CSA13 and CSA131. Furthermore,
554 knockdown of *kdsC* (56), encoding an enzyme involved in LPS biosynthesis, also led to
555 sensitivity to LL37. Knockdown strains for *rpoE*, the gene encoding the envelope stress
556 responsive sigma factor σ^E (39, 42, 43), and the ubiquinone biosynthesis gene *ubiJ* (58)
557 were sensitive to CSA13, but not to CSA131, also supporting the idea that these

558 ceragenins have distinctive mechanisms of action. On the other hand, the knockdown
559 strain for the fatty acid biosynthesis gene *fabI* (52, 53) was sensitive to both CSA13 and
560 CSA131 and not to the CAMPs, and may constitute a common molecular determinant of
561 sensitivity to ceragenins. Other genes involved in fatty acid metabolism were identified
562 as genetic interactors with CAMPs. More specifically, interference with the expression of
563 *acpP*, encoding acyl carrier protein (54), led to resistance to colistin, whereas knockdown
564 of *fabZ*, encoding a lipid dehydratase (55), led to sensitivity to LL37, demonstrating
565 differences between the mechanisms of action of these two CAMPs, as previously
566 suggested (35, 57). Taken together, these results support the notion that both CAMPs and
567 ceragenins work by similar yet distinct mechanisms. These studies also provide a starting
568 point for genetic determination of the mode of action for ceragenins.
569

DISCUSSION

Although ceragenins were originally designed to mimic the physiochemical properties of CAMPs (11, 12), our results indicate that they evoke different responses from bacteria than naturally-occurring CAMPs. The fact that they work on a broader array of microbes than CAMPs, including mycobacteria, as showed by this study, also suggests that they have different mechanisms of action. Our results showed that ceragenins target an essential and conserved feature of the cellular envelope and kill phylogenetically diverse bacteria. Using trancriptomics, proteomics and a CRISPRi genetic approach, we compared the responses of bacteria to CAMPs and ceragenins and revealed similarities, but also striking differences, and showed that ceragenins trigger a distinctive envelope stress response. Interestingly, our data also suggested that the two prototypical ceragenins, CSA13 and CSA131, trigger different responses in bacteria. Overall, while our results confirmed that ceragenins act on the bacterial envelope, they challenged the assumption that CAMPs and ceragenins share the same mechanism of action.

Although ceragenins have the ability to kill mycobacteria, their activity varies considerably among species. The physicochemical properties of the mycobacterial cell envelope influences its permeability (59) and might explain the observed differences in susceptibility to ceragenins among mycobacterial strains and species (FIG. 1). The identification of the target(s) of ceragenins may reveal an essential feature of the clinically-relevant mycobacteria.

592 The profiling of the response of *E. coli* to CAMPs and ceragenins showed that
593 these compounds trigger the Cpx envelope stress response, which is known to contribute
594 to the bacterial adaptation to defects in the secretion and folding of inner membrane and
595 periplasmic proteins (39, 60). This corroborates previous studies demonstrating that
596 CpxR/CpxA influence the susceptibility of bacteria to CAMPs (61, 62) and suggests that
597 the Cpx response might similarly help bacteria to survive exposure to ceragenins. The
598 hypothesis that the envelope stress response is induced by CAMPs and ceragenins is also
599 supported by the modulation of genes associated with cis-acting elements for σ^E (FIG. 4)
600 and by the enrichment and/or depletion of CRISPRi strains targeting components of the
601 bacterial envelope (FIG. 7).
602
603 A striking similarity between the transcriptomic profiles of bacteria exposed to
604 CAMPs and ceragenins is the downregulation of genes involved in the biosynthesis of
605 purines and pyrimidines (FIG. 2K, 3C, 3D, 4B & 5B). The cause of this downregulation
606 is unknown, but it is possible that the repression of these metabolic pathways is part of
607 the adaptive response to antibiotic exposure (63) and/or relates to a decrease requirement
608 for nucleic acid in growth-inhibited bacteria. An intriguing question is whether the flux of
609 the metabolites through these nucleotide metabolic pathways affect susceptibility to
610 antimicrobial agents targeting the bacterial envelope, as observed for other antibiotics
611 (64).
612
613 The results of this study showed that *E. coli* responds differently to CAMPs and
614 ceragenins. We showed that CAMPs specifically induced the Rcs response and the

615 expression of genes involved in the biosynthesis of colanic acid (FIG. 2J, 3A, 3B, 5C, 6C
616 and 6E). This is consistent with a previous study that demonstrated that CAMPs,
617 including polymyxin B and LL37, induce the Rcs regulon through the outer membrane
618 lipoprotein RcsF (65). Surprisingly, the ceragenins CSA13 and CSA131 did not induce
619 the Rcs response as markedly as CAMPs (FIG. 5C). In contrast with the current model
620 that outer membrane perturbation by CAMPs is required for the activation of the Rcs
621 response by RcsF (65, 66), our results show that ceragenins perturb the bacterial envelope
622 of *E. coli* without extensively triggering the Rcs response. We also found that ceragenins,
623 but not CAMPs, induced the expression of genes involved in phosphate transport and of
624 the PhoB regulon (FIG. 2J, 3A, 3B, 5D and 6D). Although the reasons why these genes
625 are differently modulated following exposure to antimicrobial compounds is not
626 understood, these results strongly suggest that ceragenins and CAMPs might have
627 distinctive mechanisms of action.
628
629 Despite some similarities between the response of bacteria exposed to ceragenins,
630 such as the upregulation of several genes of the Cpx and PhoB regulons and the
631 downregulation of genes involved in nucleotides metabolism, our data also showed
632 striking differences between bacteria exposed to CSA13 and CSA131 (FIG. 2I, 2J, 2K
633 and 7G). These differences include the upregulation of genes encompassing several
634 functions (e.g. transcription factors and proteins involved in the heat response) as well as
635 the downregulation of genes involved in protein translation in bacteria exposed to CSA13
636 (FIG. 2J and 2K). The cause of these differences is unknown, however, as noted above,
637 the LogP values of CSA13 and CSA131 differ by almost 2 orders of magnitude. Given

638 that the site of action is the bacterial envelope, such significant difference in coefficient
639 partition values is likely to alter responses to membrane targets. Future work exploring
640 the response of bacteria to a broader range of ceragenins will help in understanding these
641 differences and might help in the design of compounds with a more defined mode of
642 action.
643
644 Our CRISPRi approach identified sensitizing interactions between genes involved
645 in the biology of the bacterial envelope and the antibacterial compounds colistin, LL37,
646 CSA13 and CSA131 (FIG.7). This information might prove valuable for the design of
647 combination therapies that are synergistic and prevent the emergence of resistance, but
648 also allow treatment regimens with lower concentrations of antibiotics and dose-related
649 antibiotic toxicity (67-69). As an example, trilosan, a compound inhibiting the ceragenin-
650 sensitivity determinant FabI (70) (FIG. 7G), might synergize with ceragenins. In addition,
651 the CAMPs/ceragenins-sensitivity determinant LpxB was suggested as a target for the
652 development of antibacterial compounds (71), which compounds would have the
653 potential to more broadly synergize with CAMPs and ceragenins (FIG. 7G). Although
654 those antibacterial interactions are purely speculative, our results suggest that the
655 CRISPRi approach presented here constitutes a platform for target identification and the
656 development of antibiotic combination therapies.
657
658 The results of this study suggested that CAMPs and ceragenins both kill bacteria
659 by targeting the bacterial envelope. However, this study also supports the hypothesis that
660 ceragenins have a distinctive mode of action and we propose a model in which ceragenins

cross the outer layers of the bacterial envelope and disrupt the inner membrane. This hypothesis is supported by the broad spectrum of action of these molecules, which extend beyond bacteria. Whether the broader activity range of ceragenins impacts the selectivity for microbial membranes characteristic of endogenous CAMPs remains a key question for future study. A better understanding of the structure-activity relationship of these compounds and a deeper knowledge of their unique mechanism of action will be essential in the discovery of the next-generation of ceragenins with increased potency and selectivity.

ACKNOWLEDGEMENTS

The authors would like to thank Teresa Repasy and Guillaume Golovkine for their assistance during the design of the RNAseq experiments, and Daniel A. Portnoy for providing *L. monocytogenes* 10403S. We acknowledge help from the UC Berkeley Functional Genomics Laboratory, the UC Davis Genome Center and the UC Davis Bioinformatics Core in performing and analyzing RNAseq experiments as well as the Chan Zuckerberg Biohub for the sequencing of the CRISPRi libraries. The UC Berkeley proteomics core provided assistance with the LC-MS analysis of our peptide samples. J.M.B was supported by NIH training grants (4T32HL007185-39 & -40; 5K12HL119997-05; 1K08AI146267-0) and a Cystic Fibrosis Foundation Harry Shwachman Award during the course of this study. This work was supported by the Ceragenin Research Fund granted to M.A.M. and J.S.C. by Bill Brown and Sharon Bonner-Brown.

683 **REFERENCES**

684 1. World Health Organization. 2014. Antimicrobial resistance: global report on surveillance
685 2014. World Health Organization, Geneva, Switzerland.
686 2. World Health Organization. 2019. Global tuberculosis report 2019. World Health
687 Organization, Geneva, Switzerland.
688 3. Coates AR, Halls G, Hu Y. 2011. Novel classes of antibiotics or more of the same? Br J
689 Pharmacol 163:184-94.
690 4. Silver LL. 2011. Challenges of antibacterial discovery. Clin Microbiol Rev 24:71-109.
691 5. Tommasi R, Brown DG, Walkup GK, Manchester JI, Miller AA. 2015. ESKAPEing the
692 labyrinth of antibacterial discovery. Nat Rev Drug Discov 14:529-42.
693 6. Bradshaw J. 2003. Cationic antimicrobial peptides : issues for potential clinical use.
694 BioDrugs 17:233-40.
695 7. Brogden KA. 2005. Antimicrobial peptides: pore formers or metabolic inhibitors in
696 bacteria? Nat Rev Microbiol 3:238-50.
697 8. Sochacki KA, Barns KJ, Bucki R, Weisshaar JC. 2011. Real-time attack on single
698 Escherichia coli cells by the human antimicrobial peptide LL-37. Proc Natl Acad Sci U S A
699 108:E77-81.
700 9. Omardien S, Brul S, Zaat SA. 2016. Antimicrobial Activity of Cationic Antimicrobial
701 Peptides against Gram-Positives: Current Progress Made in Understanding the Mode of
702 Action and the Response of Bacteria. Front Cell Dev Biol 4:111.
703 10. Pfalzgraff A, Brandenburg K, Weindl G. 2018. Antimicrobial Peptides and Their
704 Therapeutic Potential for Bacterial Skin Infections and Wounds. Front Pharmacol 9:281.
705 11. Hashemi MM, Holden BS, Durnas B, Bucki R, Savage PB. 2017. Ceragenins as mimics of
706 endogenous antimicrobial peptides. J Antimicrob Agents 3.
707 12. Li C, Peters AS, Meredith EL, Allman GW, Savage PB. 1998. Design and Synthesis of
708 Potent Sensitizers of Gram-Negative Bacteria Based on a Cholic Acid Scaffolding. J Am
709 Chem Soc 120:2961-2962.
710 13. Piktel E, Levental I, Durnas B, Janmey PA, Bucki R. 2018. Plasma Gelsolin: Indicator of
711 Inflammation and Its Potential as a Diagnostic Tool and Therapeutic Target. Int J Mol Sci
712 19.
713 14. Pollard JE, Snarr J, Chaudhary V, Jennings JD, Shaw H, Christiansen B, Wright J, Jia W,
714 Bishop RE, Savage PB. 2012. In vitro evaluation of the potential for resistance
715 development to ceragenin CSA-13. J Antimicrob Chemother 67:2665-72.
716 15. Epand RF, Pollard JE, Wright JO, Savage PB, Epand RM. 2010. Depolarization, bacterial
717 membrane composition, and the antimicrobial action of ceragenins. Antimicrob Agents
718 Chemother 54:3708-13.
719 16. Li C, Budge LP, Driscoll CD, Willardson BM, Allman GW, Savage PB. 1999. Incremental
720 conversion of outer-membrane permeabilizers into potent antibiotics for Gram-negative
721 bacteria. . J Am Chem Soc 121:931-940.
722 17. Guan Q, Li C, Schmidt EJ, Boswell JS, Walsh JP, Allman GW, Savage PB. 2000. Preparation
723 and characterization of cholic acid-derived antimicrobial agents with controlled
724 stabilities. Org Lett 2:2837-40.
725 18. Lim B, Miyazaki R, Neher S, Siegele DA, Ito K, Walter P, Akiyama Y, Yura T, Gross CA.
726 2013. Heat shock transcription factor sigma32 co-opts the signal recognition particle to
727 regulate protein homeostasis in E. coli. PLoS Biol 11:e1001735.

19. Becavin C, Bouchier C, Lechat P, Archambaud C, Creno S, Gouin E, Wu Z, Kuhbacher A, Brisse S, Pucciarelli MG, Garcia-del Portillo F, Hain T, Portnoy DA, Chakraborty T, Lecuit M, Pizarro-Cerda J, Moszer I, Bierne H, Cossart P. 2014. Comparison of widely used Listeria monocytogenes strains EGD, 10403S, and EGD-e highlights genomic variations underlying differences in pathogenicity. mBio 5:e00969-14.
20. Champion PA, Champion MM, Manzanillo P, Cox JS. 2009. ESX-1 secreted virulence factors are recognized by multiple cytosolic AAA ATPases in pathogenic mycobacteria. Mol Microbiol 73:950-62.
21. Snapper SB, Melton RE, Mustafa S, Kieser T, Jacobs WR, Jr. 1990. Isolation and characterization of efficient plasmid transformation mutants of Mycobacterium smegmatis. Mol Microbiol 4:1911-9.
22. Otero J, Jacobs WR, Jr., Glickman MS. 2003. Efficient allelic exchange and transposon mutagenesis in Mycobacterium avium by specialized transduction. Appl Environ Microbiol 69:5039-44.
23. Clinical and Laboratory Standards Institute. 2018. Methods for dilution antimicrobial susceptibility tests for bacteria that grow aerobically. Approved standard. 11th edition. Clinical and Laboratory Standards Institute, Wayne, PA.
24. Lamontagne Boulet M, Isabelle C, Guay I, Brouillette E, Langlois JP, Jacques PE, Rodrigue S, Brzezinski R, Beauregard PB, Bouarab K, Boyapelly K, Boudreault PL, Marsault E, Malouin F. 2018. Tomatidine Is a Lead Antibiotic Molecule That Targets Staphylococcus aureus ATP Synthase Subunit C. Antimicrob Agents Chemother 62.
25. Ritchie ME, Phipson B, Wu D, Hu Y, Law CW, Shi W, Smyth GK. 2015. limma powers differential expression analyses for RNA-sequencing and microarray studies. Nucleic Acids Res 43:e47.
26. Huang da W, Sherman BT, Lempicki RA. 2009. Bioinformatics enrichment tools: paths toward the comprehensive functional analysis of large gene lists. Nucleic Acids Res 37:1-13.
27. Huang DW, Sherman BT, Lempicki RA. 2009. Systematic and integrative analysis of large gene lists using DAVID Bioinformatics Resources. Nature Protoc 4:44-57.
28. Bioinformatics and Evolutionary Genomics. Calculate and draw custom Venn diagrams. http://bioinformatics.psb.ugent.be/webtools/Venn/. Accessed 2020-02-01.
29. Huerta AM, Glasner JD, Gutiérrez-Ríos RM, Blattner FR, Collado-Vides J. 2002. GETools: gene expression tool for analysis of transcriptome experiments in E. coli. Trends in Genetics 18:217-218.
30. Santos-Zavaleta A, Salgado H, Gama-Castro S, Sanchez-Perez M, Gomez-Romero L, Ledezma-Tejeida D, Garcia-Sotelo JS, Alquicira-Hernandez K, Muniz-Rascado LJ, Pena-Loredo P, Ishida-Gutierrez C, Velazquez-Ramirez DA, Del Moral-Chavez V, Bonavides-Martinez C, Mendez-Cruz CF, Galagan J, Collado-Vides J. 2019. RegulonDB v 10.5: tackling challenges to unify classic and high throughput knowledge of gene regulation in E. coli K-12. Nucleic Acids Res 47:D212-D220.
31. Budzik JM, Swaney DL, Jimenez-Morales D, Johnson JR, Garelis NE, Repasy T, Roberts AW, Popov LM, Parry TJ, Pratt D, Ideker T, Krogan NJ, Cox JS. 2020. Dynamic post-translational modification profiling of M. tuberculosis-infected primary macrophages. Elife 9.
32. Cox J, Mann M. 2008. MaxQuant enables high peptide identification rates, individualized p.p.b.-range mass accuracies and proteome-wide protein quantification. Nat Biotechnol 26:1367-72.

33. Jimenez-Morales D, Campos AR, Von Dollen J. 2019. artMS: Analytical R tools for Mass Spectrometry. https://bioconductor.org/packages/release/bioc/html/artMS.html. Accessed 2020-02-01.
34. Choi M, Chang CY, Clough T, Broudy D, Killeen T, MacLean B, Vitek O. 2014. MSstats: an R package for statistical analysis of quantitative mass spectrometry-based proteomic experiments. Bioinformatics 30:2524-6.
35. Pristovsek P, Kidric J. 1999. Solution structure of polymyxins B and E and effect of binding to lipopolysaccharide: an NMR and molecular modeling study. J Med Chem 42:4604-13.
36. Dominguez A, Munoz E, Lopez MC, Cordero M, Martinez JP, Vinas M. 2017. Transcriptomics as a tool to discover new antibacterial targets. Biotechnol Lett 39:819-828.
37. Briffotaux J, Liu S, Gicquel B. 2019. Genome-Wide Transcriptional Responses of Mycobacterium to Antibiotics. Front Microbiol 10:249.
38. Price NL, Raivio TL. 2009. Characterization of the Cpx regulon in Escherichia coli strain MC4100. J Bacteriol 191:1798-815.
39. Mitchell AM, Silhavy TJ. 2019. Envelope stress responses: balancing damage repair and toxicity. Nat Rev Microbiol 17:417-428.
40. Jishage M, Iwata A, Ueda S, Ishihama A. 1996. Regulation of RNA polymerase sigma subunit synthesis in Escherichia coli: intracellular levels of four species of sigma subunit under various growth conditions. J Bacteriol 178:5447-51.
41. Sun Z, Cagliero C, Izard J, Chen Y, Zhou YN, Heinz WF, Schneider TD, Jin DJ. 2019. Density of sigma70 promoter-like sites in the intergenic regions dictates the redistribution of RNA polymerase during osmotic stress in Escherichia coli. Nucleic Acids Res 47:3970-3985.
42. Erickson JW, Gross CA. 1989. Identification of the sigma E subunit of Escherichia coli RNA polymerase: a second alternate sigma factor involved in high-temperature gene expression. Genes Dev 3:1462-71.
43. Alba BM, Gross CA. 2004. Regulation of the Escherichia coli sigma-dependent envelope stress response. Mol Microbiol 52:613-9.
44. Nonaka G, Blankschien M, Herman C, Gross CA, Rhodius VA. 2006. Regulon and promoter analysis of the E. coli heat-shock factor, sigma32, reveals a multifaceted cellular response to heat stress. Genes Dev 20:1776-89.
45. Rolfes RJ, Zalkin H. 1988. Escherichia coli gene purR encoding a repressor protein for purine nucleotide synthesis. Cloning, nucleotide sequence, and interaction with the purF operator. J Biol Chem 263:19653-61.
46. Cho BK, Federowicz SA, Embree M, Park YS, Kim D, Palsson BO. 2011. The PurR regulon in Escherichia coli K-12 MG1655. Nucleic Acids Res 39:6456-64.
47. Lamarche MG, Wanner BL, Crepin S, Harel J. 2008. The phosphate regulon and bacterial virulence: a regulatory network connecting phosphate homeostasis and pathogenesis. FEMS Microbiol Rev 32:461-73.
48. Silvis MR, Gross CA. In preparation.
49. Peters JM, Colavin A, Shi H, Czarny TL, Larson MH, Wong S, Hawkins JS, Lu CHS, Koo BM, Marta E, Shiver AL, Whitehead EH, Weissman JS, Brown ED, Qi LS, Huang KC, Gross CA. 2016. A Comprehensive, CRISPR-based Functional Analysis of Essential Genes in Bacteria. Cell 165:1493-1506.

50. Metzger LEt, Raetz CR. 2009. Purification and characterization of the lipid A disaccharide synthase (LpxB) from Escherichia coli, a peripheral membrane protein. Biochemistry 48:11559-71.
51. Narita S, Tokuda H. 2009. Biochemical characterization of an ABC transporter LptBFGC complex required for the outer membrane sorting of lipopolysaccharides. FEBS Lett 583:2160-4.
52. Bergler H, Fuchsbichler S, Hogenauer G, Turnowsky F. 1996. The enoyl-[acyl-carrier-protein] reductase (FabI) of Escherichia coli, which catalyzes a key regulatory step in fatty acid biosynthesis, accepts NADH and NADPH as cofactors and is inhibited by palmitoyl-CoA. Eur J Biochem 242:689-94.
53. Heath RJ, Rock CO. 1995. Enoyl-acyl carrier protein reductase (fabI) plays a determinant role in completing cycles of fatty acid elongation in Escherichia coli. J Biol Chem 270:26538-42.
54. Rawlings M, Cronan JE, Jr. 1992. The gene encoding Escherichia coli acyl carrier protein lies within a cluster of fatty acid biosynthetic genes. J Biol Chem 267:5751-4.
55. Heath RJ, Rock CO. 1996. Roles of the FabA and FabZ beta-hydroxyacyl-acyl carrier protein dehydratases in Escherichia coli fatty acid biosynthesis. J Biol Chem 271:27795-801.
56. Biswas T, Yi L, Aggarwal P, Wu J, Rubin JR, Stuckey JA, Woodard RW, Tsodikov OV. 2009. The tail of KdsC: conformational changes control the activity of a haloacid dehalogenase superfamily phosphatase. J Biol Chem 284:30594-603.
57. Turner J, Cho Y, Dinh NN, Waring AJ, Lehrer RI. 1998. Activities of LL-37, a cathelin-associated antimicrobial peptide of human neutrophils. Antimicrob Agents Chemother 42:2206-14.
58. Hajj Chehade M, Pelosi L, Fyfe CD, Loiseau L, Rascalou B, Brugiere S, Kazemzadeh K, Vo CD, Ciccone L, Aussel L, Coute Y, Fontecave M, Barras F, Lombard M, Pierrel F. 2019. A Soluble Metabolon Synthesizes the Isoprenoid Lipid Ubiquinone. Cell Chem Biol 26:482-492 e7.
59. Jackson M. 2014. The mycobacterial cell envelope-lipids. Cold Spring Harb Perspect Med 4.
60. Raivio TL. 2014. Everything old is new again: an update on current research on the Cpx envelope stress response. Biochim Biophys Acta 1843:1529-41.
61. Audrain B, Ferrieres L, Zairi A, Soubigou G, Dobson C, Coppee JY, Beloin C, Ghigo JM. 2013. Induction of the Cpx envelope stress pathway contributes to Escherichia coli tolerance to antimicrobial peptides. Appl Environ Microbiol 79:7770-9.
62. Weatherspoon-Griffin N, Zhao G, Kong W, Kong Y, Morigen, Andrews-Polymenis H, McClelland M, Shi Y. 2011. The CpxR/CpxA two-component system up-regulates two Tat-dependent peptidoglycan amidases to confer bacterial resistance to antimicrobial peptide. J Biol Chem 286:5529-39.
63. Zampieri M, Zimmermann M, Claassen M, Sauer U. 2017. Nontargeted Metabolomics Reveals the Multilevel Response to Antibiotic Perturbations. Cell Rep 19:1214-1228.
64. Yang JH, Wright SN, Hamblin M, McCloskey D, Alcantar MA, Schrubbers L, Lopatkin AJ, Satish S, Nili A, Palsson BO, Walker GC, Collins JJ. 2019. A White-Box Machine Learning Approach for Revealing Antibiotic Mechanisms of Action. Cell 177:1649-1661 e9.
65. Farris C, Sanowar S, Bader MW, Pfuetzner R, Miller SI. 2010. Antimicrobial peptides activate the Rcs regulon through the outer membrane lipoprotein RcsF. J Bacteriol 192:4894-903.

868 66. Konovalova A, Mitchell AM, Silhavy TJ. 2016. A lipoprotein/beta-barrel complex
869 monitors lipopolysaccharide integrity transducing information across the outer
870 membrane. Elife 5.
871 67. Zheng W, Sun W, Simeonov A. 2018. Drug repurposing screens and synergistic drug-
872 combinations for infectious diseases. Br J Pharmacol 175:181-191.
873 68. Zimmermann GR, Lehar J, Keith CT. 2007. Multi-target therapeutics: when the whole is
874 greater than the sum of the parts. Drug Discov Today 12:34-42.
875 69. Moellering RC, Jr. 1983. Rationale for use of antimicrobial combinations. Am J Med 75:4-
876 8.
877 70. Heath RJ, Rubin JR, Holland DR, Zhang E, Snow ME, Rock CO. 1999. Mechanism of
878 triclosan inhibition of bacterial fatty acid synthesis. J Biol Chem 274:11110-4.
879 71. Bohl TE, Shi K, Lee JK, Aihara H. 2018. Crystal structure of lipid A disaccharide synthase
880 LpxB from Escherichia coli. Nat Commun 9:377.

881

FIGURE LEGENDS

FIGURE 1. Ceragenins kills phylogenetically diverse bacteria. (A) Structures of the ceragenins CSA13 and CSA131. Minimal inhibitory concentrations (MIC) of colistin (COL), LL37, CSA13, CSA131 and ciprofloxacin (CIP) against *E. coli* MG1655 (B), *L. monocytogenes* (Lmo) 10403S (C), *M. avium* $mc^2$2500 (D), *M. avium* $mc^2$2500D6 (E), *M. marinum* M strain (F), *M. smegmatis* $mc^2$155 (G) and *M. tuberculosis* Erdman (H). Dots and bars indicate results from independent experiments and median values, respectively. Time-kill experiments of *E. coli* MG1655 (I), *L. monocytogenes* 10403S (J) and *M. smegmatis* $mc^2$155 (K) exposed to colistin (in red), LL37 (in blue), CSA13 (in yellow), CSA131 (in green), ciprofloxacin (in purple) and/or erythromycin (ERY; in orange), a bacteriostatic antibiotic. Untreated samples are in black and results are showed as means of two independent experiments. Shaded areas show standard error of the mean (SEM). Serial passages of *E. coli* (L) and *L. monocytogenes* (M) exposed to CSA13 (in yellow), CSA131 (in green) and ciprofloxacin (in purple). Bacteria were passaged daily in presence of sub-inhibitory concentrations of antibiotics. Results are expressed as means and SEM of two independent experiments.

FIGURE 2. Transcriptomic response of *E. coli* exposed to ceragenins. RNA from exponentially growing *E. coli* bacteria exposed to supra-MIC concentrations of colistin (COL), LL37, CSA13 and CSA131 was extracted and sequenced. (A-D) Replica plots showing the $\log_{10}$ of normalized number of reads per gene for bacteria exposed to antibiotics. Correlation coefficients (R) between replicates #1 and #2 (●) and #1 and #3 (●) are displayed. (E-H) Volcano plots that represent RNA expression as means of $\log_2$

fold changes and -$\log_{10}$ adjusted P_{values} (adj. P_{value}) for bacteria exposed to antibiotics in comparison to untreated control samples. Horizontal and vertical dotted red lines indicate adjusted *P* values less than 0.05 (or -$\log_{10}$ (adj. P_{value}) greater than 1.3) and absolute $\log_2$ fold changes greater than 1. (I) Multidimensional scaling (MDS) plot showing the separation between biological replicates and between untreated and antibiotic-treated samples. (J) Annotation terms enriched for genes significantly up-regulated ($\log_2$ FC > 1 and adj. P_{value} < 0.05) following exposure to antibiotics. (K) Annotation terms enriched for genes significantly down-regulated ($\log_2$ FC < -1 and adj. P_{value} < 0.05) following exposure to antibiotics. Adjusted P_{values} of annotation terms associated with a false discovery rate (FDR) value > 0.05 for at least one antibiotic are showed. Only the 8 most statistically significant annotation terms are showed for each conditions. Annotation terms are abbreviated and/or modified for a purpose of presentation (see Data Set S2 for a more detailed information). Data are from 3 independent experiments.

FIGURE 3. Identification of pathways defining the transcriptional response of *E. coli* to ceragenins. (A) Venn diagram analysis of genes significantly up-regulated ($\log_2$ FC > 1 and adjusted P_{value} < 0.05) in *E. coli* exposed to antibiotics. Annotation terms associated with a false discovery rate (FDR) value > 0.05 for genes up-regulated by all antibiotics, by CAMPs or by ceragenins are shown by dotted arrows. (B) Top 25 most up-regulated genes for bacteria exposed to all antibiotics, to CAMPs or to ceragenins. Genes belonging to the annotation terms «signal» (in red), «LPS», «colanic acid», «slime layer» and «exopolysaccharide» (in blue) and «phosphate transport» (in green) are indicated. (C) Venn diagram analysis of genes significantly down-regulated ($\log_2$ FC < -1

928 and adjusted $P_{value} < 0.05$) in *E. coli* exposed to antibiotics. Annotation terms associated
929 with a false discovery rate (FDR) value > 0.05 for genes down-regulated by all
930 antibiotics, by CAMPs or by ceragenins are shown by dotted arrows. (D) Top 25 most
931 down-regulated genes for bacteria exposed to all antibiotics or to ceragenins. Genes
932 belonging to the annotation terms «de novo IMP», «de novo UMP», «purine» and
933 «pyrimidine» (in orange) and «oligo/dipeptide transport» (in purple) are indicated.
934 Annotation terms are abbreviated and/or modified for the purpose of presentation (see
935 Data Set S3 for a more detailed information). Data are from 3 independent experiments.
936
937 **FIGURE 4. Identification of cis-acting elements that regulate the transcriptional**
938 **response of *E. coli* to ceragenins.** Genes with known or predicted promoters or binding
939 sites for transcription factors are enumerated for genes commonly up-regulated (A) or
940 down-regulated (B) by all antibiotics (black bars), by CAMPs (red bars) or by ceragenins
941 (in blue). Only promoters/binding sites identified more than once for at least one group
942 are represented.
943
944 **FIGURE 5. Expression of the CpxR, PurR, RcsA and PhoB regulons in *E. coli***
945 **exposed to ceragenins.** Heat maps of $\log_2$ fold changes for genes of the CpxR (A), PurR
946 (B), RcsA (C) and PhoB (D) regulons in bacteria exposed to antibiotics. Genes predicted
947 to be induced (in black), repressed (in blue) or both (in orange) by a specific transcription
948 factors are indicated. Data are from 3 independent experiments.
949

FIGURE 6. Proteomic response of *E. coli* exposed to colistin and CSA13. (A) Number of unique proteins identified for each conditions. (B) Correlation coefficient (R) between the number of peptides per proteins between the biological replicates of untreated bacteria and bacteria exposed to colistin (COL) or CSA13. Data are represented as means and standard deviations. (C-D) Volcano plots that represent protein expression as means of $\log_2$ fold changes and -$\log_{10}$ adjusted P_{values} (adj. P_{value}) for bacteria exposed to antibiotics in comparison to untreated controls. Horizontal and vertical dotted red lines indicate adjusted *P* values less than 0.05 (or -$\log_{10}$ (adj. P_{value}) greater than 1.3) and absolute $\log_2$ fold changes greater than 1. Some proteins that are members of the Cpx regulon (in red), involved in colanic acid biosynthesis (in blue) or members of the PhoB regulon (in green) are highlighted. (E) Annotation terms enriched for proteins significantly up- or down-regulated (absolute $\log_2$ FC > 1 and adj. $P_{value} < 0.05$) following the exposure of *E. coli* to colistin and CSA13. Adjusted P_{values} of annotation terms associated with a false discovery rate (FDR) value > 0.05 for at least one antibiotic are showed. Annotation terms are abbreviated and/or modified for the purpose of presentation (see Data Set S6 for a more detailed information). Data are from 3 independent bacterial cultures for each conditions.

FIGURE 7. Identification of the genetic determinants of resistance to ceragenins in *E. coli*. (A) Details and calibration of the *E. coli* CRISPRi system. dCas9 and sgRNA expression cassettes were integrated into the chromosome (Tn7att and lambda att, respectively) and controlled by weak constitutive (dcas9) or inducible (sgRNA) promoters, as indicated. Right panels show that CRISPRi produces unimodal reduction in

973 expression when targeting chromosomal *rfp* (i.e. a gene encoding a red fluorescent
974 protein). Median percentages of knockdown are indicated in the right lower panel. (B)
975 Schematic of the pooled growth experiments of *E. coli* CRISPRi libraries in the presence
976 or absence of antibacterial compounds. The strain-specific metrics of fitness and
977 sensitivity (drug-specific) are calculated as the change in relative abundance of each
978 strain between the two time points or conditions, using the formulae as indicated.
979 Changes in abundance (Log_2FC) and adjusted P_{values} ($-Log_{10}$(adj. P_{value})) associated with
980 each strain following exposure to colistin (COL) (C), LL37 (D), CSA13 (E) and CSA131
981 (F) are shown. Horizontal and vertical dotted red lines indicate adjusted *P* values less
982 than 0.05 (or $-\log_{10}$ (adj. P_{value}) greater than 1.3) and absolute $\log_2$ fold changes greater
983 than 0.5. Genes associated with significant changes in abundance are labeled for each
984 compounds. (G) Mean fold changes in abundance and standard deviations (SD)
985 associated with significantly enriched or depleted CRISPRi strains (only one *rpoE*-
986 targeting strain is shown) following exposure to COL, LL37, CSA13 and CSA131 (*, $P <$
987 0.05 [Two-tailed unpaired *t*-test]). Means and SDs were calculated from counts
988 normalized to the total number of counts for each conditions. Data are from two
989 biological replicates.
990
991

SUPPLEMENTAL MATERIALS

Supplement Table S1. Minimal inhibitory concentrations (MIC) of colistin, LL37, CSA13, CSA131, CSA44, CSA144 and ciprofloxacin against *E. coli*, *L. monocytogenes* and *Mycobacterium* spp.

Supplement Figure S1. Supplementary information related to CRISPRi screening. Schematic of two examples of deep sequencing libraries from the strategy used to multiplex growth experiments using 50bp single end reads. Each library is barcoded using aTruSeq i7 index (orange), and additionally incorporates a 4bp barcode (teal) that is read out by the TruSeq Read 1 primer. Each index (i7 and 4bp barcode) is introduced by the sequencing library PCR primers, enabling easy multiplexing. Library A incorporates a random offset at the start of Read 1 (NN) to ensure sequence diversity during cluster generation.

Data Set S1. Transcriptomic response of *E. coli* exposed to colistin, LL37, CSA13 and CSA131 as determined by RNAseq. This file includes raw and normalized read counts, fold changes, *P* and adjusted *P* values as well as lists of genes significantly up- or down-regulated.

Data Set S2. Annotation term enrichment analysis for significantly up- and down-regulated genes in *E. coli* exposed to colistin, LL37, CSA13 and CSA131. The analysis was performed with the DAVID Bioinformatics Resources using terms from UniProt keywords, COG ontology, GO and the KEGG pathway.

Data Set S3. Lists and annotation term enrichment analysis of genes significantly up- and down-regulated in *E. coli* exposed to all antibiotics, CAMPs and ceragenins. The analysis

1014 was performed with the DAVID Bioinformatics Resources using terms from UniProt
1015 keywords, COG ontology, GO and the KEGG pathway.
1016 **Data Set S4**. Analysis of cis-acting elements associated with genes significantly up- and
1017 down-regulated in *E. coli* exposed to colistin, LL37, CSA13 and CSA131. This file
1018 includes lists of genes with a least one binding site for sigma factors or transcription
1019 factors as well as numbers of non-redundant binding sites for each conditions. Fold
1020 changes for genes of the CpxR, PurR, RcsA and PhoB regulons are also included.
1021 **Data Set S5.** Proteomic response of *E. coli* exposed to colistin and CSA13. This file
1022 includes fold changes and adjusted *P* values (including imputed values) as well as lists of
1023 proteins significantly up- and down-regulated following exposure to colistin and CSA13.
1024 **Data Set S6.** Annotation term enrichment analysis for proteins up- and down-regulated in
1025 *E. coli* exposed to colistin or CSA13. The analysis was performed with the DAVID
1026 Bioinformatics Resources using terms from UniProt keywords, COG ontology, GO and
1027 the KEGG pathway.
1028 **Data Set S7.** Changes in abundance and statistical significance associated with each
1029 strains of the CRISPRi library following exposure to colistin, LL37, CSA13 and
1030 CSA131.

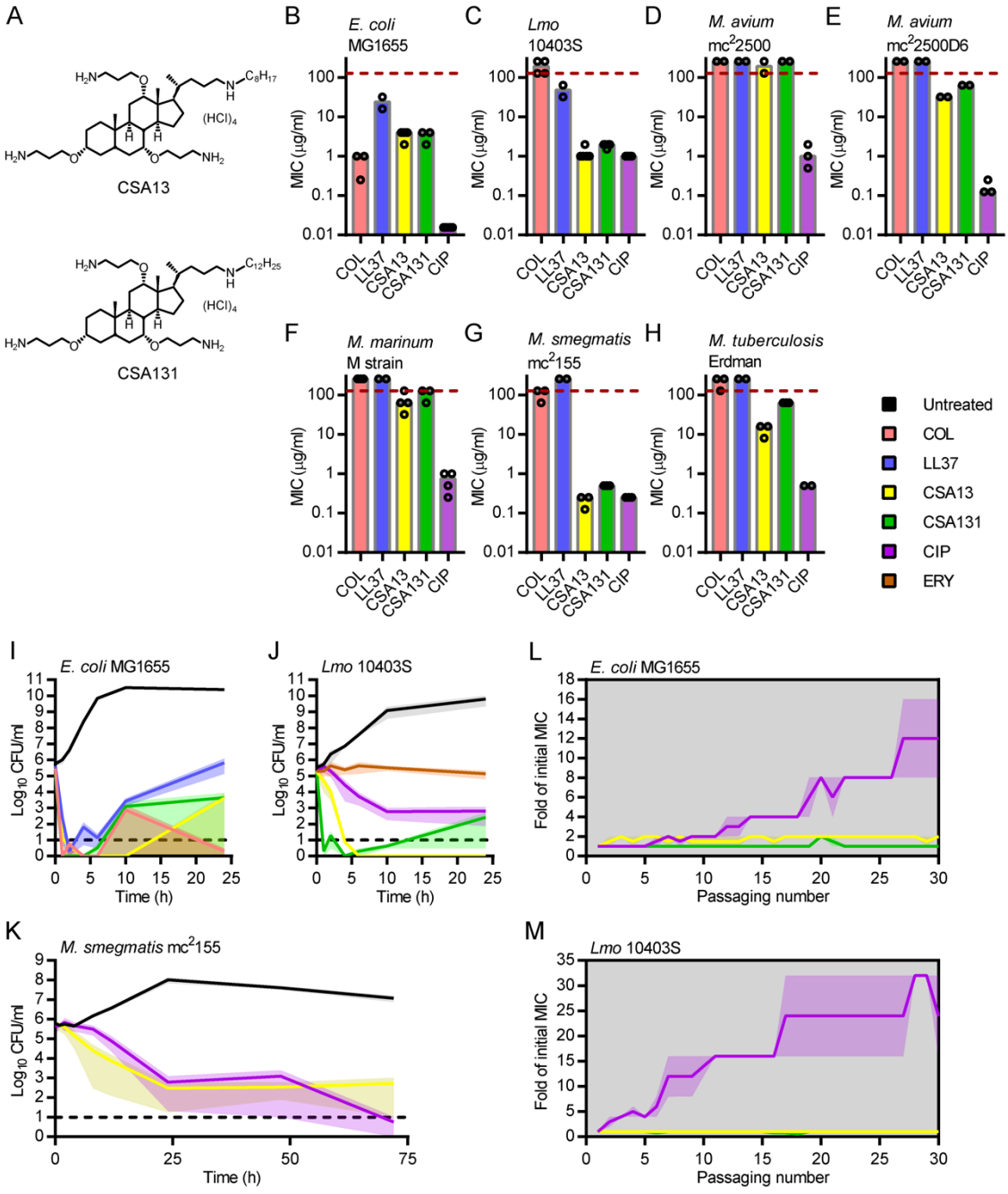

FIGURE 1.

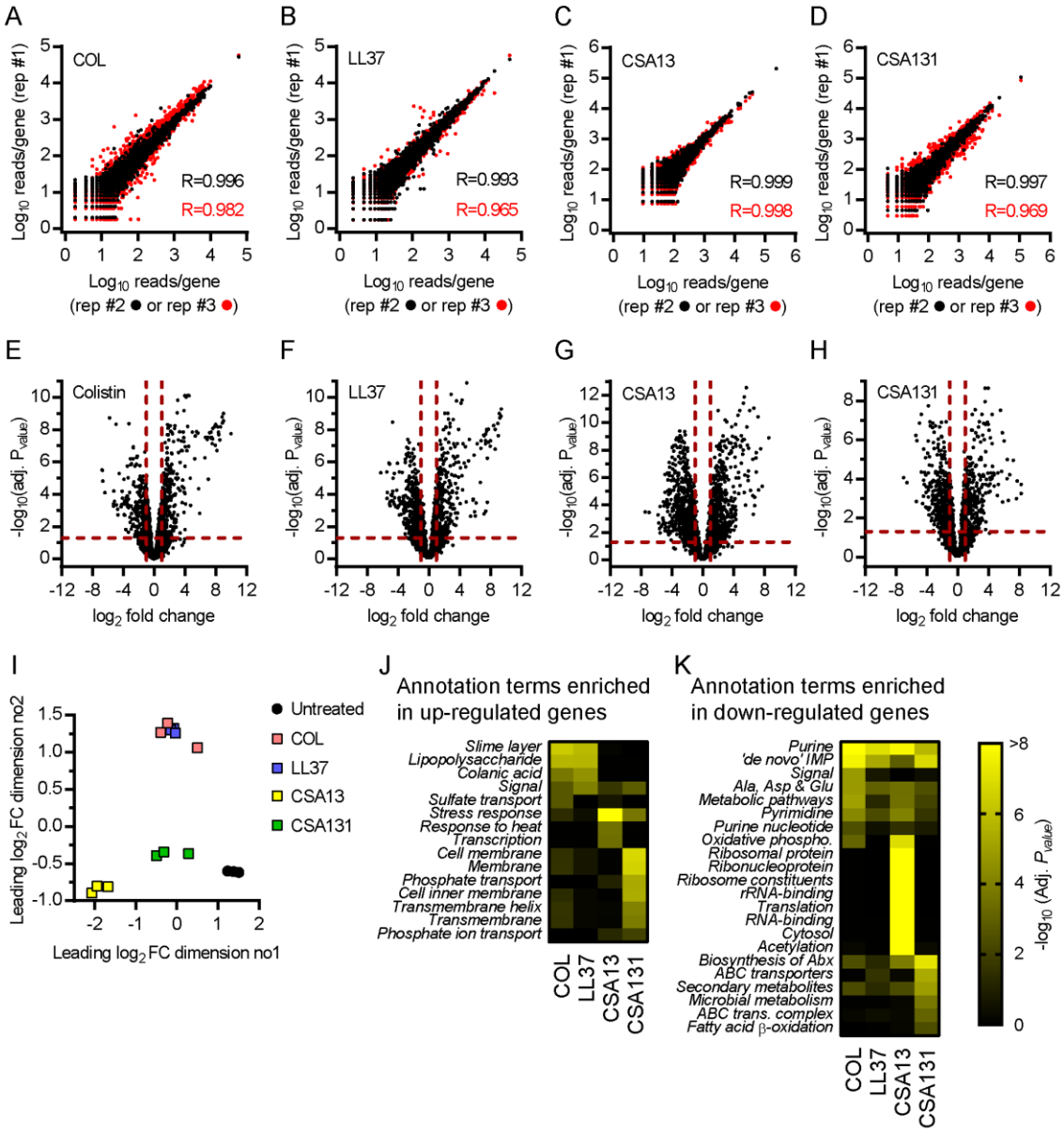

FIGURE 2.

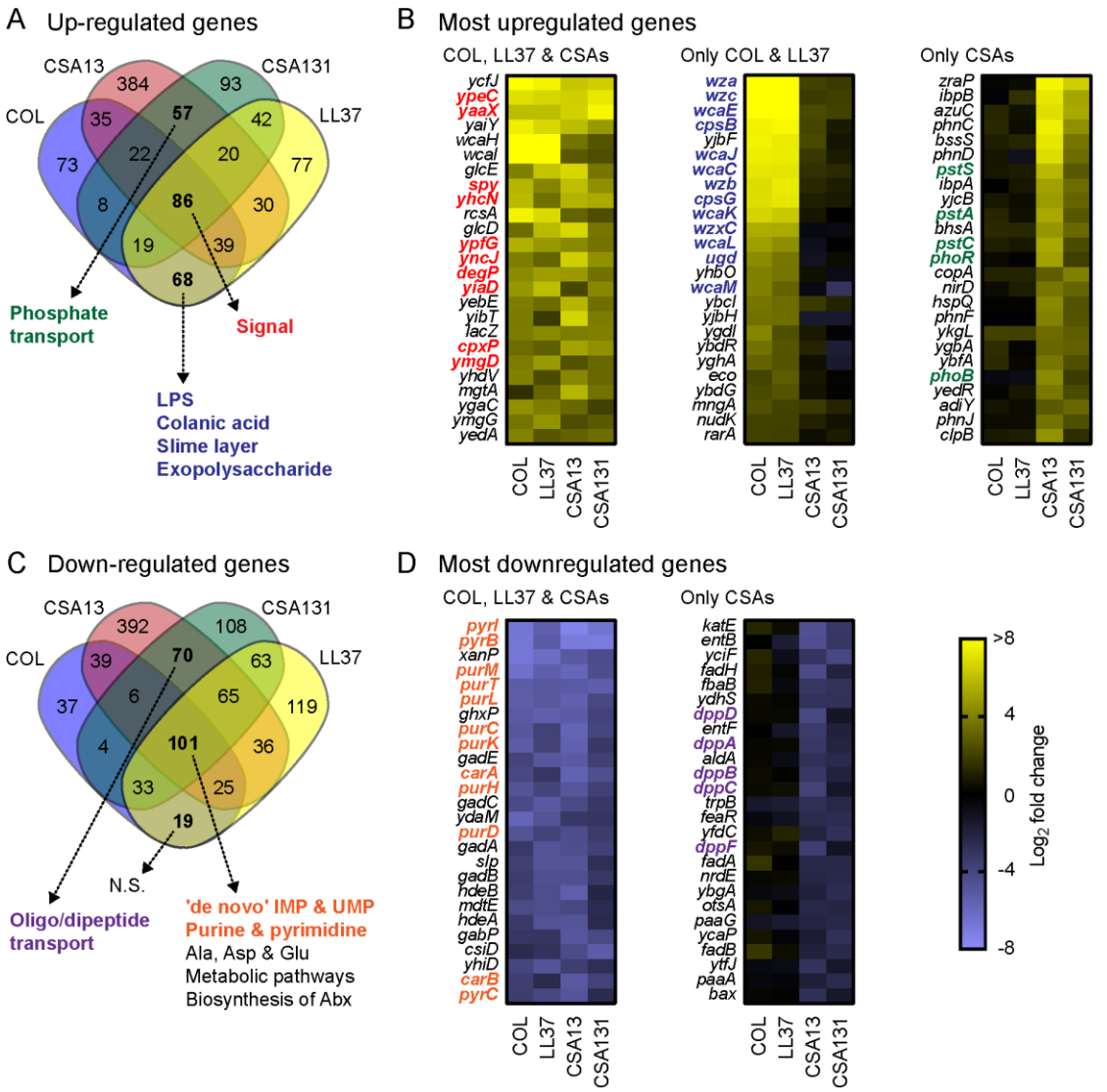

FIGURE 3.

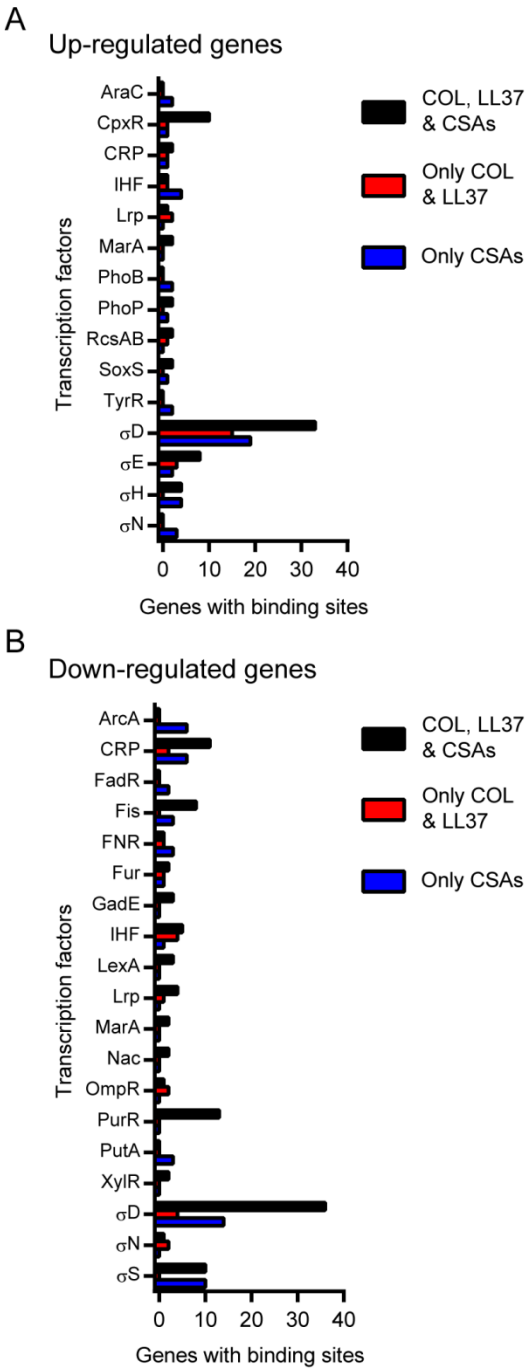

FIGURE 4.

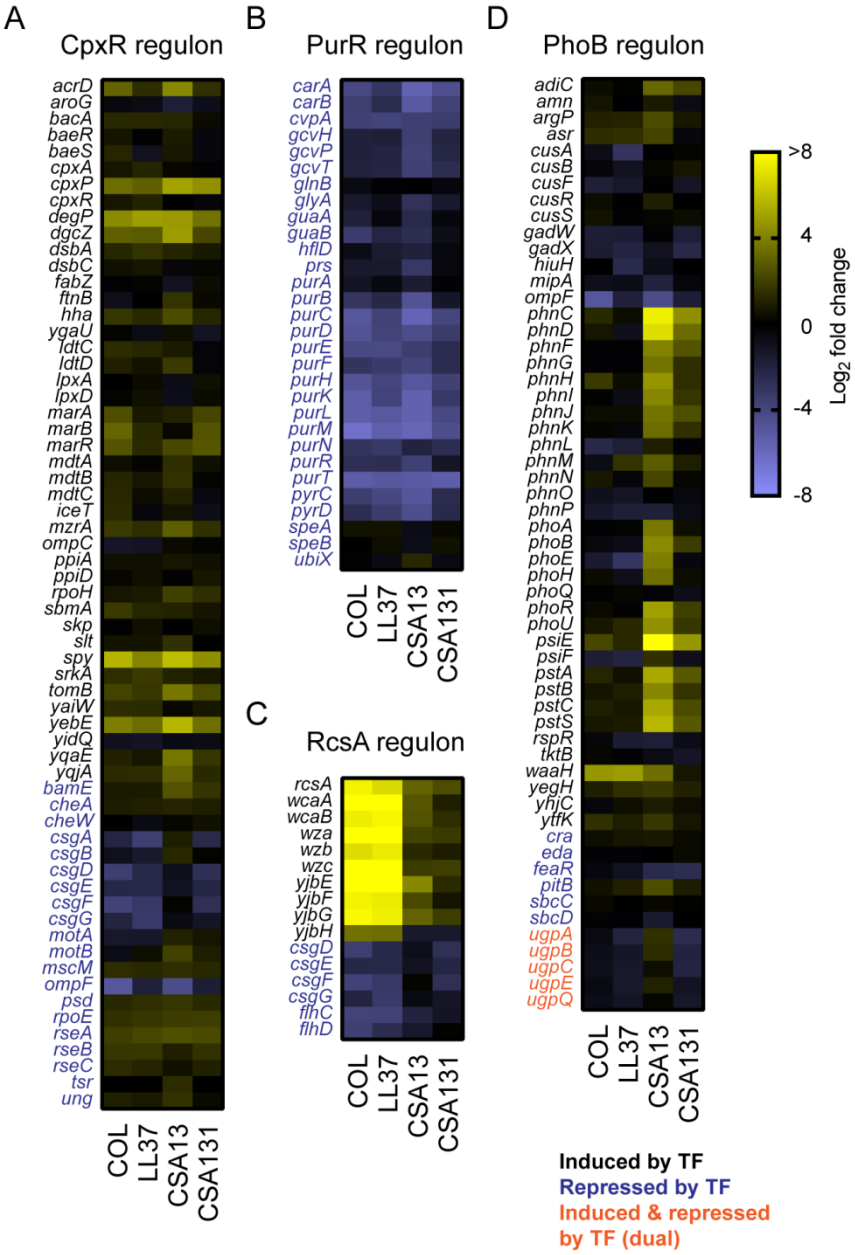

FIGURE 5

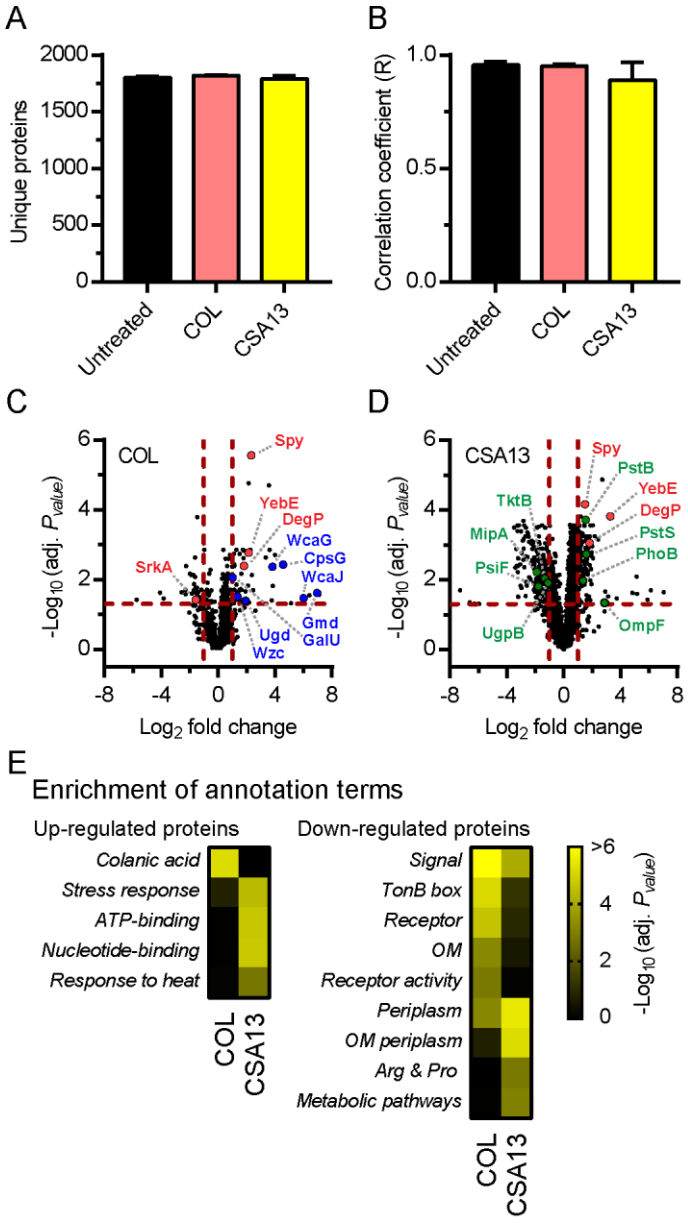

FIGURE 6.

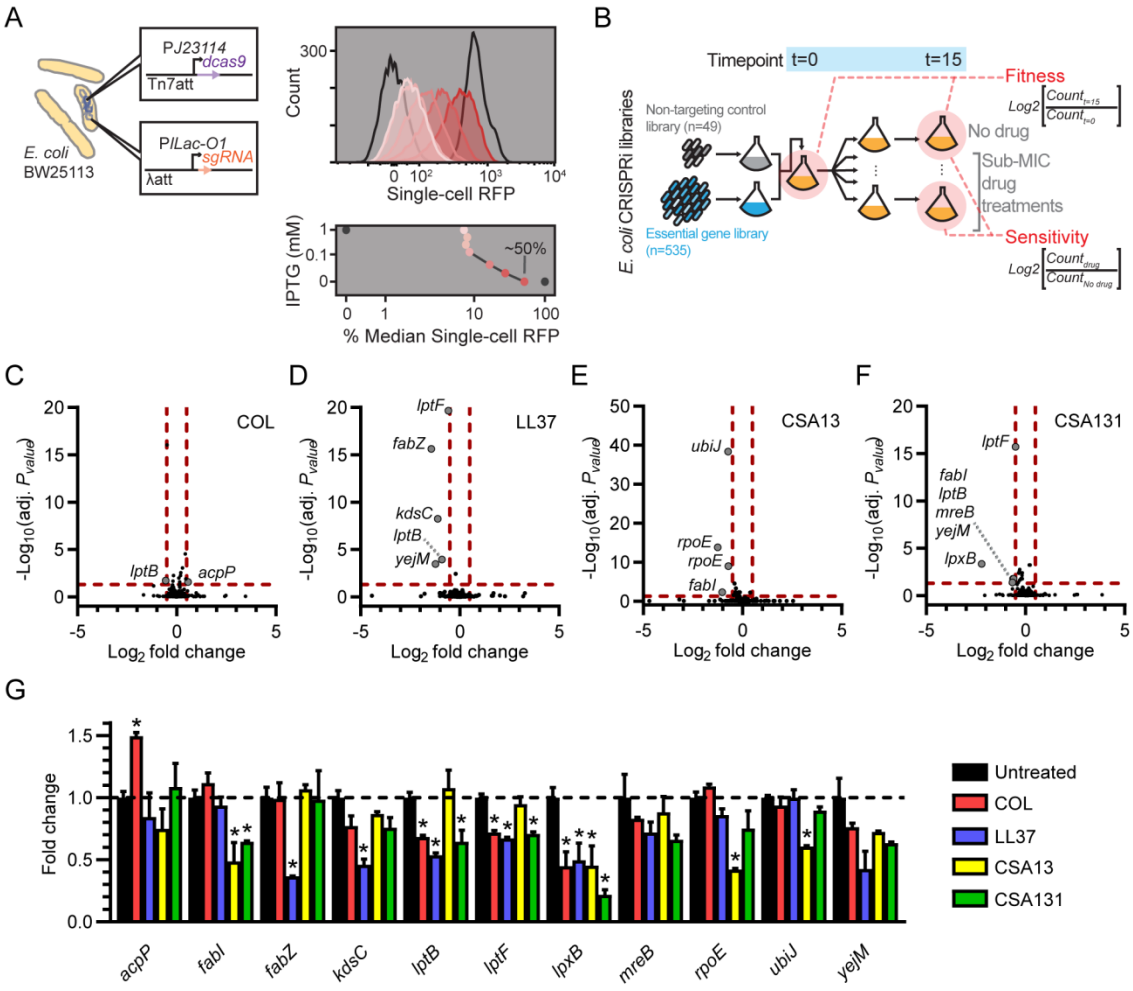

FIGURE 7.